Article

Calcium Signaling in Endocardial and Epicardial Ventricular Myocytes from Streptozotocin-Induced Diabetic Rat

Al Kury, Lina T., Sydorenko, Vadym, Smail, Manal MA, Qureshi, Muhammad A., Shmygol, Anatoly, Papandreou, Dimitrios and Singh, Jaipaul

http://dx.doi.org/10.1111/jdi.13451

DR. LINA AL KURY (Orcid ID : 0000-0002-8338-7655)

Article type : Original Article

Manuscript Category: Original Article

Calcium Signaling in Endocardial and Epicardial Ventricular Myocytes from Streptozotocin-Induced Diabetic Rat

Lina T. Al Kury [a*], Vadym Sydorenko [b], Manal MA Smail [c], Muhammad A. Qureshi [c], Anatoly Shmygol [c], Dimitrios Papandreou [a], Jaipaul Singh [d], Frank Christopher Howarth[c]

[a] Dept. of Health Sciences, College of Natural and Health Sciences, Zayed University, Abu Dhabi, UAE

[b] Dept. of Cellular Membranology, Bogomoletz Institute of Physiology, Kiev, Ukraine; vadym.sydorenko@gmail.com

[c] Dept. of Physiology, College of Medicine & Health Sciences, Al Ain, UAE University, UAE

[e] School of Forensic & Applied Sciences, University of Central Lancashire, Preston, United Kingdom

Correspondence:
Lina T. Al Kury
Department of Health Sciences, College of Natural and Health Sciences, Zayed University, Abu Dhabi 144534, UAE, email: Lina.AlKury@zu.ac.ae, Tel: +971506623975.

Running Title: Calcium transport in the diabetic heart.

Word Count: 3,480 (excluding references, supporting information, tables and figures).

ABSTRACT

Aims/Introduction: Abnormalities in Ca^{2+} signaling have a key role in hemodynamic dysfunction in diabetic heart. The purpose of this study was to explore the effects of streptozotocin

(STZ) - induced diabetes on Ca^{2+} signaling in epicardial (EPI) and endocardial (ENDO) cells of the left ventricle, after 5-6 months of STZ injection. **Materials and Methods:** Whole-cell patch clamp was used to measure L-type Ca^{2+} channel (LTCC) and Na^{+}/Ca^{2+} exchanger (NCX) currents. Fluorescence photometry techniques were used to measure intracellular free Ca^{2+} concentration $[Ca^{2+}]_i$. **Results:** Although LTCC current was not significantly altered, the amplitude (AMP) of Ca^{2+} transients increased significantly in EPI-STZ and ENDO-STZ compared to controls. Time to peak (TPK) LTCC current, TPK Ca^{2+} transient, time to half (THALF) decay of LTCC current and THALF decay of Ca^{2+} transients were not significantly changed in EPI-STZ and ENDO-STZ myocytes compared to controls. NCX current was significantly smaller in EPI-STZ and in ENDO-STZ compared to controls. **Conclusions:** STZ-induced diabetes resulted in an increase in AMP of Ca^{2+} transients in EPI and ENDO myocyte that was independent of LTCC current. Such an effect can be attributed, at least in part, to the dysfunction of NCX. Additional studies are warranted to improve our understanding of the regional impact of diabetes on Ca^{2+} signaling, which will facilitate the discovery of new targeted treatments for diabetic cardiomyopathy.

KEYWORDS: Streptozotocin-induced diabetes; ventricular myocytes; Ca^{2+} transients; L-type Ca^{2+} channel; Na^{+}/Ca^{2+} exchanger

INTRODUCTION

Cardiac contractility is controlled by variations in the concentration of intracellular free Ca^{2+} $[Ca^{2+}]_i$. During the process of excitation-contraction coupling (ECC), depolarization of the ventricular myocyte causes the opening of measure L-type Ca^{2+} channel (LTCCs) and the influx of small amounts of Ca^{2+} into the cardiac cell. This influx of Ca^{2+} stimulates a large release of Ca^{2+} (Ca^{2+} transient) from the sarcoplasmic reticulum (SR) via the ryanodine receptors (RyR) resulting in a transient rise of intracellular $[Ca^{2+}]$ (Ca^{2+} transient). Ca^{2+} attaches to troponin C which initiates and regulates the process of myocyte contraction. During the process of myocyte relaxation Ca^{2+} is removed from the cytoplasm through four main pathways: the uptake of Ca^{2+} into the SR through SR Ca^{2+}-ATPase (SERCA pump), efflux of Ca^{2+} from the cell primarily via the Na^{+}/Ca^{2+} exchanger (NCX), and to a lesser extent the Ca^{2+}-ATPase in the plasma membrane (1) and also uptake of Ca^{2+} by the mitochondria (2, 3).

Disturbances in the mechanism(s) of Ca^{2+} signaling will inevitably have implications for cardiac myocyte contraction. Previous studies in left ventricle cells obtained from the STZ-treated rat have shown alterations in the Ca^{2+} transient including prolonged TPK (4, 5), prolonged THALF relaxation (6), and unaltered (7) or reduced (8) amplitude of Ca^{2+} transient. These alterations in Ca^{2+} transient may be attributed variously to diminished SR Ca^{2+} content, release and uptake (9-11), reduced activity of L-type Ca^{2+} channel (12-14) and NCX (7, 13).

Supporting these findings, earlier studies on STZ-treated rats have variously reported reduced cardiac output, fractional shortening and ejection fraction (4, 14, 15). In cardiac cells isolated from STZ-treated rat, there was prolonged time course of shortening (6, 16, 17), frequently prolonged relaxation (4, 16) and slowed velocity of shortening and re-lengthening (14). Studies have also shown either no significant change (6, 12) or reduction (14) in the amplitude of shortening. These different results could be partly attributed to duration of diabetes or methodology employed in the experiments.

It is well known that the electromechanical characteristics of cardiac cells across the ventricular walls are different. This heterogeneity is partly attributed to distinctive expression of different ion channels and associated ionic currents which lead to variation in action potential waveforms seen in epicardial (EPI), midmyocardial (mid) and endocardial (ENDO) cells (18-20). For example, *in vivo* echocardiographic studies in rat ventricular myocardium have shown that layers of the epicardium contract less and slower than the layers of the sub-endocardium (21). It is important to highlight that any disruption in the differential distribution of ion channels responsible for Ca^{2+} transport across the walls of the ventricles is expected to be involved in the dysfunction of cardiac cells in disease (7, 15, 22, 23). Earlier work in spontaneously hypertensive rat has shown transmurally altered time course and amplitude of action potential, variation in Ca^{2+} transients and contraction in sub-EPI and sub-ENDO myocytes during compensated hypertrophy (24). Transmural alteration in the activity of NCX, Ca^{2+} content of the SR and AMP of Ca^{2+} transient have also been shown in an earlier study in spontaneously hypertensive rat (25).

To date, only a few studies have explored the transmural effect of STZ-induced diabetes on Ca^{2+} signaling in ventricular myocytes (26-28). For this reason, the current work was undertaken to investigate the progressive regional effects of diabetes on ventricular myocytes. To the best of our knowledge, this is the first study that investigates the effects of STZ-induced diabetes on LTCC current simultaneously measured with Ca^{2+} transients. Previous experiments have generally measured LTCC current and Ca^{2+} transient in separate experiments. The influx of Ca^{2+} through

LTCCs is inextricably linked to the release of Ca^{2+} from the SR (Ca^{2+}-induced Ca^{2+} release). Therefore, this study has investigated the effects of STZ-induced diabetes on LTCC current simultaneously measured with intracellular [Ca^{2+}] and also NCX current in EPI and ENDO ventricular myocytes from rats 5-6 months after the induction of diabetes.

MATERIALS AND METHODS

Experimental Model

Experiments were conducted in STZ-induced diabetic rats (29, 30). A single intraperitoneal injection of STZ (60 mg/kg bodyweight) in citrate buffer was used to induced diabetes in young adult (220-250 g) male Wistar rats. Age-matched control animals were injected with citrate buffer alone. Rats were kept at 12/12 h light/dark cycle. Food and water were supplied *ad libitum*. Both control and experimental groups received standard pelleted rat chow.

Prior to each experiment, body and heart weights, in addition to non-fasting blood glucose level (OneTouch Ultra 2, LifeScan) were measured. All experiments were done 5-6 months after treatment with STZ in ENDO and EPI myocytes. Ethical approval of the work was received from the UAE University (UAEU) Animal Research Ethics Committee (UAE University, A11-15, 2015). All experiments were performed according to the institution guidelines.

Isolation of Ventricular Myocytes

Ventricular myocytes were obtained by enzymatic and mechanical dispersal techniques in accordance with previously described protocols (24, 27, 28). Animals were euthanized with a guillotine. Hearts were isolated, mounted on a Langendorff system for retrograde perfusion and perfused at 36-37 ºC with a cell isolation solution (see supporting information) (27). Perfusion flow rate was 8 ml/g $heart^{-1}.min^{-1}$. Upon stabilization of heart contraction, perfusion was switched to Ca^{2+}-free cell isolation solution containing EGTA (0.1 mmol/l) for 4 min and then to cell isolation solution containing Ca^{2+} (0.05 mmol/l), type 1 collagenase (0.60 mg/ml) and type XIV protease (0.075 mg/ml) for 6 min. Upon completion of enzymatic treatment, hearts were detached from the Langendorff perfusion system and the left ventricle was further dissected as described in earlier studies (27, 28). Thin sections were carefully dissected by fine scissors from the outermost layer (EPI) and innermost layer (ENDO) of the left ventricle. The sections were gently minced and shaken in an isolation solution containing collagenase and 1% bovine serum albumin. Cells were then filtered at 4 min intervals and re-suspended in cell isolation solution that contained 0.75 mmol/l Ca^{2+}.

Simultaneous Recording of L-type Ca^{2+} Current and Ca^{2+} Transient

Simultaneous recording of LTCC current and Ca^{2+} transients were measured in EPI and ENDO ventricular cells according to modifications of previously described methods (27, 28, 31). All experiments were conducted at 34 ˚C. LTCC current was measured with an Axopatch 200B amplifier. Analog signal was filtered using a four-pole Bessel filter (bandwidth of 5 kHz) and digitized at a sampling rate of 10 kHz using a Digidata 1550 digitizer. The voltage clamp protocols, and data acquisition were controlled by WinWCP 4.05 software. Patch pipettes were made from filamented borosilicate glass. Resistance of electrodes was 2-4 MΩ. Seal resistances were 1–5 GΩ. Current–voltage (I-V) relationship was achieved by the application of 300 ms test pulses (-30 to +50 mV) in 10 mV steps from a holding potential of -40 mV. Intracellular Ca^{2+} recordings were obtained by loading the cells with 30 μM Fura-2-pentapotassium salt via the patch pipette for 5 min and excited at 360- and 380-nm wavelengths with dual LED light source, controlled by a spectrophotometry unit at 100 Hz. The fluorescence signal at 510 nm was collected through an adjustable diaphragm and a photomultiplier tube. WinWCP 4.05 software was used to sample signals at 10 kHz. All data were stored on a computer for subsequent analysis. After the subtraction of background signal, fluorescent signals were recorded as F_{360}/F_{380} (ratio of the fluorescent intensity when excited at 360 nm (F_{360}) to that when excited at 380 nm (F_{380}) and expressed as a ratio unit (RU). Whole cell bath solution and pipette solution used are described in the supporting information.

Measurement of Na^+/Ca^{2+} Exchange Current

NCX current was recorded according to modifications of previously described techniques (31) Experiments were conducted at 34 ˚C. Recording of NCX current was obtained with an Axopatch 200B amplifier using a voltage ramp protocol. Cells were held at a holding potential of -40 mV. Voltage ramps were deployed at a steady rate of 0.1 V/s from +60 mV to −100 mV. Resistance of electrodes was 3-5 MΩ. Seal resistances were 1–5 GΩ. Oubain (100 μM), nifedipine (10 μM) and niflumic acid (30 μM) were used to block Na^+-K^+-ATPase, Ca^{2+}, and Cl^- currents, respectively. Nickel chloride solution (10 mM) was used to block NCX. The NCX current was measured as the current sensitive to nickel (Ni^{2+}). NCX current was isolated by subtracting Ni^{2+}-insensitive component from the total current (31). Whole cell bath solution and pipette solution used are described in supporting information.

Statistical Analysis

Results were represented as mean ± S.E.M. of 'n' observations. As appropriate, independent samples t-test or one-way ANOVA followed by Bonferroni corrected t-tests were used for statistical comparisons. P value < 0.05 was considered significant.

RESULTS

General Characteristics

Bodyweight and heart weight were significantly reduced ($p<0.05$) in STZ-pretreated diabetic rats. In comparison with their respective age-matched controls, heart weight/ bodyweight and non-fasting blood glucose were greater in STZ-pretreated diabetic rats (Table 1).

Cell Capacitance

Cell capacitance was significantly lower in ENDO-STZ compared to ENDO-CON ventricular cells ($p<0.05$) (Figure 1). There was a small variation in cell capacitance between EPI-STZ and EPI-CON myocytes however, the variation was not significant ($p>0.05$).

L-type Ca^{2+} Current and Ca^{2+} Transient

Typical tracings of LTCC current and Ca^{2+} transients measured at 0 mV test potential are shown in Figure 2A. The mean current-voltage (I/V) relationship of LTCC current for ENDO-STZ, ENDO-CON, EPI-STZ and EPI-CON ventricular cells are shown in Figure 2B and the currents generated at 0 mV test voltage are represented in Figure 2C. LTCC current amplitude were not significantly ($p>0.05$) different in ENDO-STZ and EPI-STZ compared to their respective controls at 0 mV (Figure 2C). Ca^{2+} transient fura-2 ratio-voltage relationship for ENDO-STZ, ENDO-CON, EPI-STZ and EPI-CON ventricular myocytes are represented in Figure 2D. Ca^{2+} transients generated at 0 mV are represented in Figure 2E. AMP of Ca^{2+} transients were significantly ($p<0.05$) larger in ENDO-STZ and EPI-STZ compared to their controls (Figure 2E). TPK LTCC current (Figure 2F) and TPK Ca^{2+} transient (Figure 2G) were not significantly ($p>0.05$) different in ENDO-STZ and EPI-STZ compared to their respective controls ($p>0.05$). THALF decay of LTCC current (Figure 2H) and THALF decay of the Ca^{2+} transient (Figure 2I) were not significantly ($p<0.05$) in ENDO-STZ and EPI-STZ compared to their respective controls.

Na^+/Ca^{2+} Exchange Current

The current of NCX was recorded by applying a voltage ramp between +60 and -100 mV. The NCX current was calculated as the difference between current generated in presence of 10 μM nifedipine and current in presence of nifedipine and 10 mM Ni^{2+}. Mean recordings of ramp current in ENDO-CON, ENDO-STZ, EPI-CON and EPI-STZ ventricular cells are represented in Figure 3A. At +60 mV, the amplitude of NCX current was significantly ($p<0.05$) smaller in ENDO-STZ and in EPI-STZ compared to their respective controls ($p<0.05$) (Figure 3B). Similarly, at -100 mV, the amplitude of NCX current was significantly ($p<0.05$) smaller in ENDO-STZ and EPI-STZ compared to their respective controls (Figure 3C).

DISCUSSION

The findings of the study show that STZ-induced diabetes causes significant alteration in Ca^{2+} transients and NCX current in EPI and ENDO ventricular myocytes. To the best of our knowledge, this is the first study to investigate the regional effects of STZ-induced diabetes on LTCC current simultaneously measured with Ca^{2+} transients and NCX current in ventricular myocytes from STZ-induced diabetic rat.

Many changes during ECC may give rise to changes in the Ca^{2+} transient. In our experiments, the AMP and the kinetics of LTCC current were similar in rat ventricular cells from EPI compared to ENDO regions. The AMP of LTCC currents were not significantly different in ENDO-STZ and EPI-STZ ventricular cells compared to their controls. Although some studies have previously reported decreased AMP (12, 32), many studieshave reported no change in LTCC currents in ventricular cells from STZ-treated rat (4, 11, 33, 34).

Interestingly, the AMP of the Ca^{2+} transients were significantly larger in EPI-STZ and ENDO-STZ myocytes compared to their respective controls. However, no regional difference in Ca^{2+} transients was observed. Earlier studies have reported either reduced (4, 15, 35) or unaltered (16, 32, 36) Ca^{2+} transients in ventricular cells, isolated from STZ-induced diabetic animals. In comparison to other studies, in which Ca^{2+} transients were measured after 3-12 weeks of STZ treatment (16, 17, 32, 33, 37), our experiments were conducted in EPI and ENDO ventricular myocytes 5-6 months after STZ treatment. Thus, the variation in results may be partly related to the degree of progression of diabetes. Furthermore, the discrepancy between our data and other results, where decreased amplitude (38) or no change in amplitude (7) of the Ca^{2+} transients were

observed, may be down to the fact that different Ca^{2+} dyes were used for intracellular Ca^{2+} recordings. In our study, a low concentration of Fura-2-pentapotassium salt was dialysed into the cell via the patch pipette. However, other studies (7, 38) have used ester of Indo-1 (Indo-1/AM) to load the indicator. Although both are high affinity indicators that have been used for cytosolic Ca^{2+} measurements in many studies in cardiac myocytes and other cell types, variation in indicator and/or loading technique may account for different results. For example, the use of Indo-1 dye is sometimes associated with overloading of cytoplasm with Ca^{2+} indicator leading to increased buffering of Ca^{2+}, slowing down the transients decay and reducing their amplitude.

The observed rise in the amplitudes of Ca^{2+} transients is explained by changes in pathways of Ca^{2+} extrusion (e.g., NCX) which, along with SERCA, are responsible for decreasing cytosolic Ca^{2+}. In our study, there was a significant decrease in NCX current in both EPI and ENDO ventricular cells, although no regional difference in the activity of NCX were observed. Earlier studies have also shown that the density of NCX current was reduced (7, 13, 39) and current inactivation was prolonged (13) in ventricular cells isolated from STZ-treated diabetic rat. These variations in the amplitude and kinetics of current were accompanied with decreased NCX mRNA (7) and reduced or unaltered NCX protein in STZ-induced diabetic rat heart (8, 11, 40). It is possible that the decrease in Ca^{2+} extrusion rate via NCX leads to a net increase in intracellular Ca^{2+} (41), increase in SR Ca^{2+} load, and as a consequence, increased cytosolic Ca^{2+} transients (11, 14, 17, 33, 42). Alternatively, the increase in the AMP of Ca^{2+} transients can be linked to ryanodine receptor (RyR) dysfunction. Abnormal function of RyR is associated with various diseases including cardiac hypertrophy and STZ-induced type 1 diabetes (43). It is known that the metabolic changes associated with diabetes stimulate the production of reactive oxygen species. As RyR structure is rich in free thiol groups, it is subject to oxidative stress, changing its tertiary structure and altering its sensitivity to Ca^{2+} (43, 44). In an earlier study in 7-week sedentary type 1 diabetic rats, the frequency of Ca^{2+} spark was three times higher, and evoked release of Ca^{2+} was dys-synchronous with the diastolic release. Although the steady-state RyR protein was not altered, its response to Ca^{2+} was changed. The RyR also displayed about 1.5 times rise in phosphorylation at Ser 2808 and Ser 2814 residues (14).

In addition to the effects observed in diabetes, earlier studies have shown that hypertension-induced cardiac hypertrophy causes an alteration in the AMP and the time course of systolic Ca^{2+} transients. Fowler et al. (2005) have shown that NCX activity is diminished while AMP of Ca^{2+} transient and SR Ca^{2+} content are increased in spontaneously hypertensive rats in comparison to

their respective controls (25). It was suggested that alteration in Ca^{2+} signaling during compensated hypertrophy is attributed to the reduction in ventricular myocyte NCX activity. As a result, SR Ca^{2+} content increases and thus, AMP of Ca^{2+} transient amplitude, serving to maintain the force of contraction against the elevated afterload (25, 45). This observation is consistent with the increased SR Ca^{2+} content of spontaneously hypertensive rat ventricular cells reported previously (46). Similarly, an increase in SR Ca^{2+} content, SR Ca^{2+} release, and AMP of Ca^{2+} transients were also described in a canine model of compensated hypertrophy that was induced by chronic AV block (47).

Earlier studies have also reported that abnormal intracellular Ca^{2+} transport is caused by the change in expression of proteins that modulate intracellular Ca^{2+}. For example, Teshima et al. (2000) have shown that expression of SERCA and RyR mRNA were significantly altered in the heart, 3 and 12 weeks post STZ injection, respectively (23). Hattori et al. (2000) have shown that the reduction in cardiac NCX activity is due to the reduction in NCX mRNA and protein 6 weeks after the induction of diabetes with STZ (7). Changes in the expression of mRNA that encodes different proteins in cardiac muscle have also been previously reported in data from our laboratory (48).

Transmural gradients in myocyte Ca^{2+} handling proteins exists across the ventricular wall. For example, it has been shown that Ca^{2+} handling proteins such as SERCA, RyR and NCX are more abundant in the EPI cells than ENDO cells in various species (49-51). Results of our study indicated that the amplitude of NCX current is larger in EPI-CON compared to END-CON. Supporting this finding, Xiong et al. (2005) reported that NCX current, protein and mRNA were greater in EPI than ENDO or MID cells (51). Wang et al. (2010) also reported transmural gradient in NCX with the capacity for Ca^{2+} extrusion by NCX being ENDO < MID < EPI (20). The spatial electrical heterogeneity of ion channels and proteins has a profound effect not only on normal cardiac electrophysiology and contractility, but also on the genesis of cardiac arrhythmias in diseased hearts. For example, the loss of this non-uniformity, has been previously reported to be a sensitive index to discriminate physiological from pathological left ventricular remodelling (21). The diminished NCX function in diabetic myocytes shown in this study suggest that NCX function may play an important role when Ca^{2+} rises to pathological levels, such as in diabetic cardiomyopathy. Furthermore, the disruption of the transmural NCX gradient in diabetic heart highlights a potential substrate for the production of lethal arrhythmias leading to heart failure in diabetic patient.

In conclusion, the present study suggests that STZ-induced diabetes causes a significant rise in Ca^{2+} transient amplitudes, 5-6 weeks after induction of diabetes with a single intraperitoneal injection of STZ. This change probably stems partly from the dysfunction of NCX. Additional studies would be needed to further our understanding of how diabetes alters Ca^{2+} handling in different regions of the heart. This will contribute to the development of new and regionally targeted treatments for diabetic cardiomyopathy.

ACKNOWLEDGMENTS

The work was funded by the College of Medicine and Health Sciences, UAE University in Al Ain; Zayed University in Abu Dhabi and Al Ain Equestrian, Shooting and Golf Club.

DISCLOSURE

The authors declare no conflict of interest.

References

1. Eisner DA, Caldwell JL, Kistamas K, Trafford AW. Calcium and Excitation-Contraction Coupling in the Heart. Circulation research. 2017;121(2):181-95.

2. Bodi I, Mikala G, Koch SE, Akhter SA, Schwartz A. The L-type calcium channel in the heart: the beat goes on. The Journal of clinical investigation. 2005;115(12):3306-17.

3. Walsh C, Barrow S, Voronina S, Chvanov M, Petersen OH, Tepikin A. Modulation of calcium signalling by mitochondria. Biochimica et biophysica acta. 2009;1787(11):1374-82.

4. Shao CH, Rozanski GJ, Patel KP, Bidasee KR. Dyssynchronous (non-uniform) Ca2+ release in myocytes from streptozotocin-induced diabetic rats. Journal of molecular and cellular cardiology. 2007;42(1):234-46.

5. Howarth FC, Almugaddum FA, Qureshi MA, Ljubisavljevic M. The effects of heavy long-term exercise on ventricular myocyte shortening and intracellular Ca2+ in streptozotocin-induced diabetic rat. J Diabetes Complications. 2010;24(4):278-85.

6. Ren J, Walsh MF, Hamaty M, Sowers JR, Brown RA. Altered inotropic response to IGF-I in diabetic rat heart: influence of intracellular Ca2+ and NO. Am J Physiol. 1998;275(3):H823-30.

7. Hattori Y, Matsuda N, Kimura J, Ishitani T, Tamada A, Gando S, et al. Diminished function and expression of the cardiac Na+-Ca2+ exchanger in diabetic rats: implication in Ca2+ overload. The Journal of physiology. 2000;527 Pt 1:85-94.

8. Lee TI, Chen YC, Kao YH, Hsiao FC, Lin YK, Chen YJ. Rosiglitazone induces arrhythmogenesis in diabetic hypertensive rats with calcium handling alteration. Int J Cardiol. 2013;165(2):299-307.

9. Lagadic-Gossmann D, Buckler KJ, Le Prigent K, Feuvray D. Altered Ca2+ handling in ventricular myocytes isolated from diabetic rats. Am J Physiol. 1996;270(5 Pt 2):H1529-37.

10. Takeda N, Dixon IM, Hata T, Elimban V, Shah KR, Dhalla NS. Sequence of alterations in subcellular organelles during the development of heart dysfunction in diabetes. Diabetes Res Clin Pract. 1996;30 Suppl:113-22.

11. Choi KM, Zhong Y, Hoit BD, Grupp IL, Hahn H, Dilly KW, et al. Defective intracellular Ca(2+) signaling contributes to cardiomyopathy in Type 1 diabetic rats. American journal of physiology Heart and circulatory physiology. 2002;283(4):H1398-408.

12. Hamouda NN, Sydorenko V, Qureshi MA, Alkaabi JM, Oz M, Howarth FC. Dapagliflozin reduces the amplitude of shortening and Ca(2+) transient in ventricular myocytes from streptozotocin-induced diabetic rats. Molecular and cellular biochemistry. 2015;400(1-2):57-68.

13. Chattou S, Diacono J, Feuvray D. Decrease in sodium-calcium exchange and calcium currents in diabetic rat ventricular myocytes. Acta physiologica Scandinavica. 1999;166(2):137-44.

14. Shao CH, Wehrens XH, Wyatt TA, Parbhu S, Rozanski GJ, Patel KP, et al. Exercise training during diabetes attenuates cardiac ryanodine receptor dysregulation. Journal of applied physiology (Bethesda, Md : 1985). 2009;106(4):1280-92.

15. Tian C, Shao CH, Moore CJ, Kutty S, Walseth T, DeSouza C, et al. Gain of function of cardiac ryanodine receptor in a rat model of type 1 diabetes. Cardiovascular research. 2011;91(2):300-9.

16. Rithalia A, Qureshi MA, Howarth FC, Harrison SM. Effects of halothane on contraction and intracellular calcium in ventricular myocytes from streptozotocin-induced diabetic rats. British journal of anaesthesia. 2004;92(2):246-53.

17. Howarth FC, Qureshi MA. Effects of carbenoxolone on heart rhythm, contractility and intracellular calcium in streptozotocin-induced diabetic rat. Mol Cell Biochem. 2006;289(1-2):21-9.

18. Remme CA, Verkerk AO, Hoogaars WM, Aanhaanen WT, Scicluna BP, Annink C, et al. The cardiac sodium channel displays differential distribution in the conduction system and transmural heterogeneity in the murine ventricular myocardium. Basic research in cardiology. 2009;104(5):511-22.

19. Abd Allah ES, Aslanidi OV, Tellez JO, Yanni J, Billeter R, Zhang H, et al. Postnatal development of transmural gradients in expression of ion channels and Ca^{2+}-handling proteins in the ventricle. Journal of molecular and cellular cardiology. 2012;53(2):145-55.

20. Wang W, Gao J, Entcheva E, Cohen IS, Gordon C, Mathias RT. A transmural gradient in the cardiac Na/K pump generates a transmural gradient in Na/Ca exchange. The Journal of membrane biology. 2010;233(1-3):51-62.

21. Aït Mou Y, Reboul C, Andre L, Lacampagne A, Cazorla O. Late exercise training improves non-uniformity of transmural myocardial function in rats with ischaemic heart failure. Cardiovascular research. 2009;81(3):555-64.

22. Lu Z, Jiang YP, Xu XH, Ballou LM, Cohen IS, Lin RZ. Decreased L-type Ca2+ current in cardiac myocytes of type 1 diabetic Akita mice due to reduced phosphatidylinositol 3-kinase signaling. Diabetes. 2007;56(11):2780-9.

23. Teshima Y, Takahashi N, Saikawa T, Hara M, Yasunaga S, Hidaka S, et al. Diminished expression of sarcoplasmic reticulum Ca(2+)-ATPase and ryanodine sensitive Ca(2+)Channel mRNA in streptozotocin-induced diabetic rat heart. Journal of molecular and cellular cardiology. 2000;32(4):655-64.

24. McCrossan ZA, Billeter R, White E. Transmural changes in size, contractile and electrical properties of SHR left ventricular myocytes during compensated hypertrophy. Cardiovascular research. 2004;63(2):283-92.

25. Fowler MR, Naz JR, Graham MD, Bru-Mercier G, Harrison SM, Orchard CH. Decreased Ca2+ extrusion via Na+/Ca2+ exchange in epicardial left ventricular myocytes during compensated hypertrophy. American journal of physiology Heart and circulatory physiology. 2005;288(5):H2431-8.

26. Casis O, Gallego M, Iriarte M, Sanchez-Chapula JA. Effects of diabetic cardiomyopathy on regional electrophysiologic characteristics of rat ventricle. Diabetologia. 2000;43(1):101-9.

27. Smail MM, Qureshi MA, Shmygol A, Oz M, Singh J, Sydorenko V, et al. Regional effects of streptozotocin-induced diabetes on shortening and calcium transport in epicardial and endocardial myocytes from rat left ventricle. Physiological reports. 2016;4(22).

28. Al Kury L, Sydorenko V, Smail MMA, Qureshi MA, Shmygol A, Oz M, et al. Voltage dependence of the Ca(2+) transient in endocardial and epicardial myocytes from the left ventricle of Goto-Kakizaki type 2 diabetic rats. Molecular and cellular biochemistry. 2018;446(1-2):25-33.

29. Szkudelski T. Streptozotocin-nicotinamide-induced diabetes in the rat. Characteristics of the experimental model. Exp Biol Med (Maywood). 2012;237(5):481-90.

30. Cheta D. Animal models of type I (insulin-dependent) diabetes mellitus. J Pediatr Endocrinol Metab. 1998;11(1):11-9.

31. Al Kury LT, Yang KH, Thayyullathil FT, Rajesh M, Ali RM, Shuba YM, et al. Effects of endogenous cannabinoid anandamide on cardiac Na(+)/Ca(2)(+) exchanger. Cell Calcium. 2014;55(5):231-7.

32. Bracken N, Howarth FC, Singh J. Effects of streptozotocin-induced diabetes on contraction and calcium transport in rat ventricular cardiomyocytes. Annals of the New York Academy of Sciences. 2006;1084:208-22.

33. Yaras N, Ugur M, Ozdemir S, Gurdal H, Purali N, Lacampagne A, et al. Effects of diabetes on ryanodine receptor Ca release channel (RyR2) and Ca2+ homeostasis in rat heart. Diabetes. 2005;54(11):3082-8.

34. Arikawa M, Takahashi N, Kira T, Hara M, Saikawa T, Sakata T. Enhanced inhibition of L-type calcium currents by troglitazone in streptozotocin-induced diabetic rat cardiac ventricular myocytes. Br J Pharmacol. 2002;136(6):803-10.

35. Moore CJ, Shao CH, Nagai R, Kutty S, Singh J, Bidasee KR. Malondialdehyde and 4-hydroxynonenal adducts are not formed on cardiac ryanodine receptor (RyR2) and sarco(endo)plasmic reticulum Ca2+-ATPase (SERCA2) in diabetes. Mol Cell Biochem. 2013;376(1-2):121-35.

36. Hamouda NN, Qureshi MA, Alkaabi JM, Oz M, Howarth FC. Reduction in the amplitude of shortening and Ca(2+) transient by phlorizin and quercetin-3-O-glucoside in ventricular myocytes from streptozotocin-induced diabetic rats. Physiological research. 2016;65(2):239-50.

37. Yaras N, Bilginoglu A, Vassort G, Turan B. Restoration of diabetes-induced abnormal local Ca2+ release in cardiomyocytes by angiotensin II receptor blockade. Am J Physiol Heart Circ Physiol. 2007;292(2):H912-20.

38. Lee MJ, Lee HS, Park SD, Moon HI, Park WH. Leonurus sibiricus herb extract suppresses oxidative stress and ameliorates hypercholesterolemia in C57BL/6 mice and TNF-alpha induced expression of adhesion molecules and lectin-like oxidized LDL receptor-1 in human umbilical vein endothelial cells. Bioscience, biotechnology, and biochemistry. 2010;74(2):279-84.

39. Lacombe VA, Viatchenko-Karpinski S, Terentyev D, Sridhar A, Emani S, Bonagura JD, et al. Mechanisms of impaired calcium handling underlying subclinical diastolic dysfunction in diabetes. American journal of physiology Regulatory, integrative and comparative physiology. 2007;293(5):R1787-97.

40. Zhang L, Ward ML, Phillips AR, Zhang S, Kennedy J, Barry B, et al. Protection of the heart by treatment with a divalent-copper-selective chelator reveals a novel mechanism underlying cardiomyopathy in diabetic rats. Cardiovasc Diabetol. 2013;12:123.

41. Kohajda Z, Farkas-Morvay N, Jost N, Nagy N, Geramipour A, Horvath A, et al. The Effect of a Novel Highly Selective Inhibitor of the Sodium/Calcium Exchanger (NCX) on Cardiac Arrhythmias in In Vitro and In Vivo Experiments. PLoS One. 2016;11(11):e0166041.

42. Howarth FC, Adem A, Adeghate EA, Al Ali NA, Al Bastaki AM, Sorour FR, et al. Distribution of atrial natriuretic peptide and its effects on contraction and intracellular calcium in ventricular myocytes from streptozotocin-induced diabetic rat. Peptides. 2005;26(4):691-700.

43. Gilca GE, Stefanescu G, Badulescu O, Tanase DM, Bararu I, Ciocoiu M. Diabetic Cardiomyopathy: Current Approach and Potential Diagnostic and Therapeutic Targets. Journal of diabetes research. 2017;2017:1310265.

44. Bidasee KR, Nallani K, Yu Y, Cocklin RR, Zhang Y, Wang M, et al. Chronic diabetes increases advanced glycation end products on cardiac ryanodine receptors/calcium-release channels. Diabetes. 2003;52(7):1825-36.

45. Naqvi RU, Macleod KT. Effect of hypertrophy on mechanisms of relaxation in isolated cardiac myocytes from guinea pig. Am J Physiol. 1994;267(5 Pt 2):H1851-61.

46. Brooksby P, Levi AJ, Jones JV. Investigation of the mechanisms underlying the increased contraction of hypertrophied ventricular myocytes isolated from the spontaneously hypertensive rat. Cardiovasc Res. 1993;27(7):1268-77.

47. Sipido KR, Volders PG, de Groot SH, Verdonck F, Van de Werf F, Wellens HJ, et al. Enhanced Ca(2+) release and Na/Ca exchange activity in hypertrophied canine ventricular myocytes: potential link between contractile adaptation and arrhythmogenesis. Circulation. 2000;102(17):2137-44.

48. Salem KA, Qureshi MA, Sydorenko V, Parekh K, Jayaprakash P, Iqbal T, et al. Effects of exercise training on excitation-contraction coupling and related mRNA expression in hearts of Goto-Kakizaki type 2 diabetic rats. Molecular and cellular biochemistry. 2013;380(1-2):83-96.

49. Currie S, Quinn FR, Sayeed RA, Duncan AM, Kettlewell S, Smith GL. Selective down-regulation of sub-endocardial ryanodine receptor expression in a rabbit model of left ventricular dysfunction. Journal of molecular and cellular cardiology. 2005;39(2):309-17.

50. Igarashi-Saito K, Tsutsui H, Takahashi M, Kinugawa S, Egashira K, Takeshita A. Endocardial versus epicardial differences of sarcoplasmic reticulum Ca2+-ATPase gene expression in the canine failing myocardium. Basic research in cardiology. 1999;94(4):267-73.

51. Xiong W, Tian Y, DiSilvestre D, Tomaselli GF. Transmural heterogeneity of Na+-Ca2+ exchange: evidence for differential expression in normal and failing hearts. Circulation research. 2005;97(3):207-9.

Table 1. General characteristics of streptozotocin-induced diabetic and age-matched control rats. Data are mean ± SEM, n=15-17 rats; ** = $p<0.05$ for diabetic compared to control.

Figure 1. Mean cell capacitance in ENDO-CON, ENDO-STZ, EPI-CON and EPI-STZ myocytes. Data are mean ± SEM, n=13-17 cells from 10-14 hearts.

Figure 2. L-type Ca^{2+} channel (LTCC) current and Ca^{2+} transient in ENDO-CON, ENDO-STZ, EPI-CON and EPI-STZ myocytes: **(a)** Typical recordings of LTCC current and Ca^{2+} transient at a test potential of 0 mV, **(b)** Mean recordings of LTCC current at test voltages in the range -30 to +50 mV, **(c)** Mean LTCC current at a test voltage of 0 mV, **(d)** Mean recordings of amplitude (AMP) of Ca^{2+} transients at test voltages in the range -30 to +50 mV, **(e)** Mean AMP of Ca^{2+} transients at a test potential of 0 mV**, (f)** TPK of LTCC current at test potentials in the range -30 to +50 mV, **(g)** TPK of Ca^{2+} transients at test potentials in the range -30 to + 50 mM, **(h)** Time to half (THALF) decay of LTCC current at test potentials in the range -30 to +50 mV, **(i)** THALF of Ca^{2+} transients at test potentials in the range -30 to +50 mV. Data are mean ± SEM, n=13-16 cells from 12-14 hearts; * = $p<0.05$.

Figure 3. Na^+/Ca^{2+} exchange current in ENDO-CON, ENDO-STZ, EPI-CON and EPI-STZ myocytes: **(a)** Mean recordings of Na^+/Ca^{2+} exchange current in (range:-100 to +60 mV), **(b)** Mean peak currents of Na^+/Ca^{2+} exchange current at +60 mV, **(c)** Mean peak currents of Na^+/Ca^{2+} exchange current at -100 mV. Data are mean ± SEM, n=14-17 cells from 9-11 hearts. * = $p<0.05$. NCX: Na^+/Ca^{2+} exchanger.

Table 1. General characteristics of streptozotocin-induced diabetic and age-matched control rats.

	Control	Streptozotocin
Bodyweight (g)	417.3±9.9	274.2±8.6**
Heart Weight (g)	1.45±0.03	1.28±0.03**
Heart weight / Body weight (mg/g)	3.50±0.07	4.68±0.10**
Non-fasting blood glucose (mg/dl)	83.3±1.31	483.9±20.2**

Data are mean ± SEM, n=15-17 rats; ** = $p<0.05$ for diabetic compared to control.

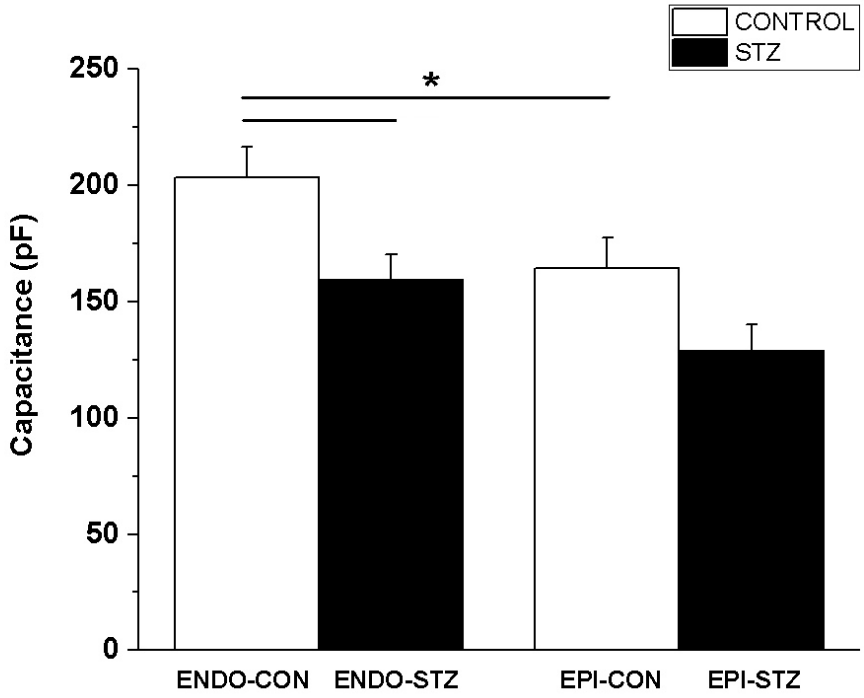

jdi_13451_f1.jpg

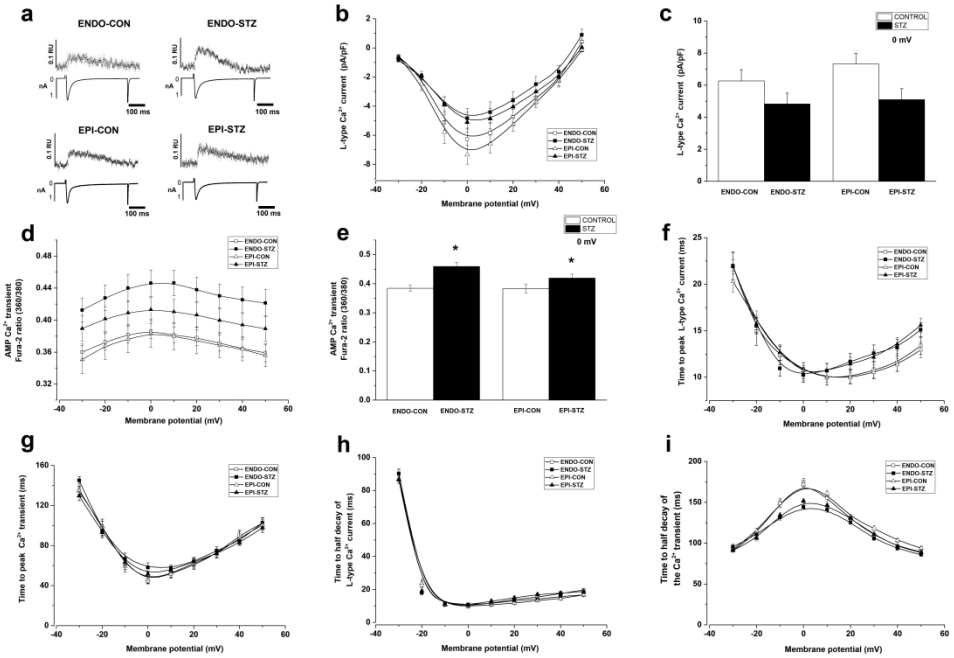

jdi_13451_f2.jpg

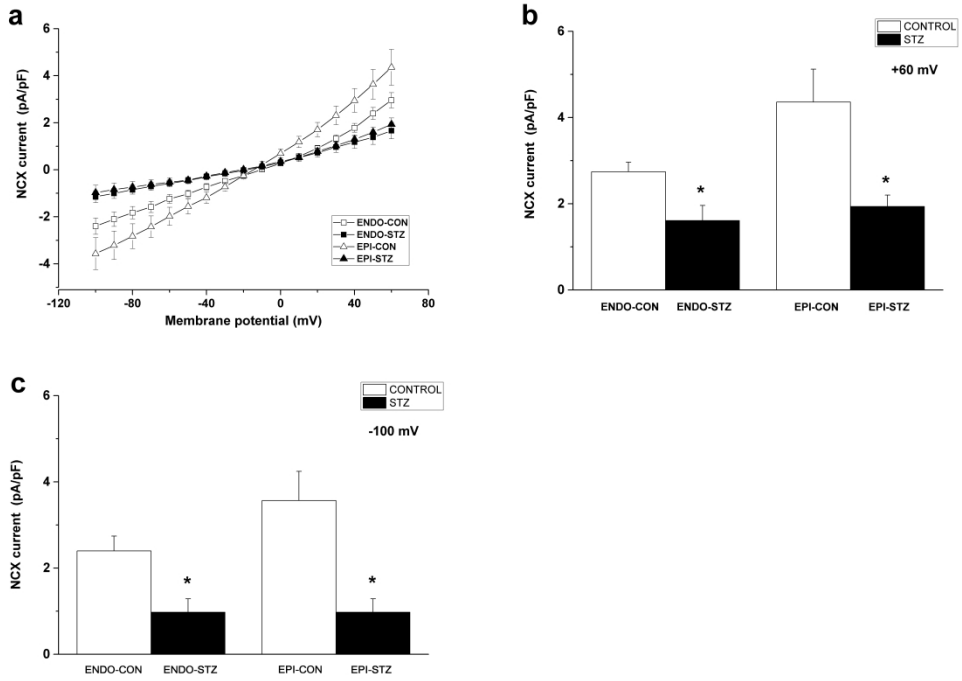

jdi_13451_f3.jpg